Published in final edited form as:
Contrast Media Mol Imaging. 2011 ; 6(1): 55–59. doi:10.1002/cmmi.395.

Self-illuminating in vivo lymphatic imaging using a bioluminescence resonance energy transfer quantum dot nano-particle

Nobuyuki Kosaka[a], **Makoto Mitsunaga**[a], **Sukanta Bhattacharyya**[b], **Steven C. Miller**[b], **Peter L. Choyke**[a], and **Hisataka Kobayashi**[a,*]

[a]Molecular Imaging Program, Center for Cancer Research, National Cancer Institute, NIH, Bethesda, MD 20892-1088, USA

[b]Zymera Inc., 5941 Optical Court, San Jose, CA 95138, USA

Abstract

Autofluorescence arising from normal tissues can compromise the sensitivity and specificity of *in vivo* fluorescence imaging by lowering the target-to-background signal ratio. Since bioluminescence resonance energy transfer quantum dot (BRET-QDot) nano-particles can self-illuminate in near-infrared in the presence of the substrate, coelenterazine, without irradiating excitation lights, imaging using BRET-QDots does not produce any autofluorescence. In this study, we applied this BRET-QDot nano-particle to the *in vivo* lymphatic imaging in mice in order to compare with BRET, fluorescence or bioluminescence lymphatic imaging. BRET-QDot655, in which QDot655 is contained as a core, was injected at different sites (e.g. chin, ear, forepaws and hind paws) in mice followed by the intravenous coelenterazine injection, and then bioluminescence and fluorescence imaging were serially performed. In all mice, each lymphatic basin was clearly visualized in the BRET imaging with minimal background signals. The BRETsignal in the lymph nodes lasted at least 30 min after coelenterazine injections. Furthermore, the BRETsignal demonstrated better quantification than the fluorescence signal emitting from QDot655, the core of this BRET particle. These advantages of BRET-QDot allowed us to perform real-time, quantitative lymphatic imaging without image processing. BRET-Qdots have the potential to be a robust nano-material platform for developing optical molecular imaging probes.

Keywords

quantum dot; nanotechnology; fluorescence; bioluminescence; lymphatic imaging; bioluminescence resonance energy transfer (BRET)

1. INTRODUCTION

In vivo optical imaging has become an important technique in biomedical imaging (1) because of its high sensitivity, low cost and feasibility for clinical translation. However, tissue autofluorescence arising from naturally occurring fluorophores can interfere with conventional *in vivo* fluorescence imaging by lowering the target to background signal ratio.

*Correspondence to: H. Kobayashi, Molecular Imaging Program, NCI/NIH, Bldg 10, Room 1B40, MSC 1088, Bethesda, MD 20892-1088, USA. Kobayash@mail.nih.gov.

3. SUPPORTING INFORMATION

Supporting information can be found in the online version of this article.

Currently, there are three strategies for overcoming autofluorescence: using near-infrared fluorophores (e.g. indocyanine green, IRDye 800CW etc.) (2) or employing ultrabright fluorophores such as quantum dots (Qdots) (3,4) or fluorescent proteins (5–7). Although these methods have successfully reduced such autofluorescence problems (8), complete elimination of autofluorescence is still difficult with *in vivo* fluorescence imaging. Another postprocessing technology is to acquire spectral images and then calculate the imaging data to remove the background signal (9). Self-illuminating bioluminescence resonance energy transfer quantum dot (BRET-Qdot) nano-particles, which do not need extrinsic excitation, represent a new strategy for eliminating background signal. They are self-illuminating with a substrate, coelenterazine, which reacts with luciferase on the BRET-Qdot. The blue bioluminescent light is efficiently transferred to the near-infrared (NIR) quantum dot core, which emits photons in the NIR without exciting autofluorescence (Figs 1 and 2) (10). This enables near-real-time bioluminescence resonance energy transfer (BRET) imaging with high target to background signal ratios but without complex and time-consuming image processing. Moreover, by changing the Qdots within BRET-Qdot, nano-particles with peak emission wavelengths of 605, 625, 655, 705 and 800 nm have been demonstrated (11). In this study, we demonstrate the feasibility of using a BRET-Qdot with 655 nm peak emission (BRET-Qdot655) for *in vivo* lymphatic imaging and evaluate the advantage of BRET-Qdot technology over conventional bioluminescence and fluorescence imaging.

For *in vivo* imaging, the BRET-Qdot technology had an advantage over conventional bioluminescence imaging (BLI) using luciferase-conjugates because the light emitted in BLI is in the blue range where tissue penetration is suboptimal. In contrast, the BRET-Qdot allows the emission of the light in the NIR with more favorable tissue penetration characteristics. As shown in the spectra in Fig. 1, although BRET-Qdot655 has both emission from luciferase in blue and Qdot in NIR *in vitro*, mostly the 655 nm NIR signal was detected in *in vivo* imaging because of the high absorbance of visible bioluminescent light in the tissue. The BRET-Qdot technology had a further advantage over conventional fluorescence imaging using Qdot or organic NIR fluorophores because it produced almost no autofluorescence, which is the largest source of background signal. Therefore, despite lower overall photon flux from BRET-Qdot655, all lymph nodes, which were reportedly depicted by the fluorescence imaging with various nano-particles (4,12–15), were visualized in all mice examined (n = 3–4 in a group; Figs. 2 and 3). In an additional set of imaging studies with a 655/40 nm band pass emission filter, which is appropriate for the Qdot655, we demonstrated that the lymph nodes were successfully depicted in spite of 80% signal loss (Supporting Information, Fig. S1), suggesting that multicolor studies with the BRET-Qdot reagents are possible. Unlike fluorescence imaging, we observed that BRET signal decreased with time (Fig. 4), probably due to the decreasing concentration of circulating coelenterazine. Despite a decreasing BRET signal, we were able to depict lymph nodes at least 30 min after a single coelenterazine injection in all mice. By changing the route of administration of coelenterazine from i.v. to local injection, prolonged depiction of the lymph node of interest was achieved up to 90 min (n = 3, Supporting Information, Fig. S2).

Additionally, for *in vivo* lymphatic imaging, because of the lack of excitation light, the BRET-Qdot655 signal more directly represents the concentration of the Qdot in the lymph node than does the fluorescence signal, even with the spectral unmixing technology, resulting in better quantitative imaging. Figure 5 shows the relative errors of *in vivo* fluorescence signal and *in vivo* BRET signal in mice injected at five sites (both forepaws, both ears and chin), when compared with *ex vivo* fluorescence signal of resected lymph nodes. In this analysis, the relative error of *in vivo* BRET imaging (0.77 ± 1.27, average ± SD) was statistically lower than that of *in vivo* fluorescence imaging (4.04 ± 7.58; p <0.005, Mann–Whitney test). This result indicates that BRET-signal can non-invasively quantify BRET-Qdot655 particles in lymph node more accurately than is typically possible with

fluorescence imaging. Fluorescence from the BRET-Qdot655 particle requires blue or green excitation light. Signal from BRET alone does not require excitation since the light is emitted from a photochemical reaction. Since the blue or green light does not sufficiently penetrate into tissues, the intensity of excitation light reaching the lymph node varies with depth, resulting in less accurate quantification of fluorescence emission.

This technology could be extended to include target-specific cancer imaging by employing a pretargeting moiety such as a biotinylated monoclonal antibody followed by a streptavidin-conjugated BRET-Qdot655. Although the dosing amounts and intervals remain to be determined, early results suggest this combination could localize target tumors (Supporting Informaiton, Fig. S3). These experiments point to a potential limitation of the BRET-Qdot system that the BRET-Qdot655 could lose its BRET signal after internalization into the cell, probably because of the catabolism of luciferase, resulting in changing luminescence performance with time. This limitation was also observed in serial *in vivo* lymphatic imaging (Supporting Informaiton, Fig. S4). Polymeric encapsulation of luciferase on BRET-Qdot particle could improve *in vivo* stability, because this modification can act as a physical barrier or compensate for the instability of the luciferase (16).

In conclusion, we demonstrate that lymphatic imaging with BRET-Qdot technology is feasible and results in images without autofluorescence. This enables the direct, real-time capture of lymphatic images without extensive image processing. Although extensive investigations including toxicity and clearance from body are required before human use, BRET-Qdots have the potential to be a robust nano-material for developing optical molecular imaging probes.

2. EXPERIMENTAL SECTION

2.1. Preparation of BRET-Qdot655 probes

BRET-Qdots®655 is commercially available from Zymera Inc. (San Jose, CA, USA). The preparation of BRET-Qdot655 probes using carboxylated Qdots (QD655, Invitrogen Corporation, Carlsbad, CA, USA) covalently linked to the Luc8 protein, an eight-mutation variant of *Renilla* luciferase, has been described (11). This BRET-Qdots655 is prepared by an optimized proprietary conjugation protocol using EDC-NHS chemistry. Briefly the conjugation is done in borate buffer at pH 7.4 and excess Luc8 (MW: 37 kDa), ethyl(dimethylaminopropyle) carbodiimide (EDC) and N-Hydroxysuccinimide (NHS) present in the reaction mixture were separated from the BRET-Qdot655 using a 100K Amicon spin filter (Millipore Corporation, Billerica, MA, USA). The purified BRET-Qdot655 conjugates (500 nM) are in 10 mM Tris buffer (pH 7.4) and are stored at 4°C. This BRET-Qdot655 product has approximately six Luc8 molecules per quantum dot based on the fluorescence and bioluminescence, which is measured using a Fluoro Max-3 Fluorometer (HORIBA Jobin Yvon Inc., Edison, NJ, USA). The hydrodynamic size of BRET-Qdot655 particles measured by dynamic light scattering (DLS) (Malvern Zeta Sizer Nano instrument, Malven Instruments Ltd, Malvern, UK) was 22 nm in diameter.

2.2. In vivo lymphatic imaging using BRET-Qdot particle

For *in vivo* lymphatic imaging using a BRET-Qdot particle, we intracutaneously injected a BRET-Qdot655 solution followed by serial imaging. All *in vivo* procedures were carried out in compliance with the Guide for the Care and Use of Laboratory Animal Resources (1996), National Research Council, and approved by the National Cancer Institute Animal Care and Use Committee. In brief, 10-week-old normal athymic female mice were anesthetized via intraperitoneal injection of 1.15 mg sodium pentobarbital (Nembutal Sodium Solution, Ovation Pharmaceuticals Inc., Deerfield, IL, USA). Mice were then administrated intracutaneous injections of 10 or 20 μL of BRET-Qdot655 solution (5 or 10 pmol,

respectively, Zymera Inc.) into different sites, whose emission light peak was 655 nm. Injected doses were 5 pmol for the chin and ear, and 10 pmol for the paws. All injection sites were masked with a nonfluorescent black tape. Within 5 min after injections, *in vivo* spectral fluorescence imaging was carried out using a spectral fluorescence imaging system (Maestro, CRi Inc., Woburn, MA, USA) with a 445–490 nm bandpass filter for excitation and a 515 nm long pass filter for emission light. Immediately after obtaining spectral fluorescence images, the mice were received intravenous injection of 10 μg of coelenterazine (Coelenterazine-h, Zymera Inc.) from a tail vein, and then *in vivo* BRET imaging was carried out using a highly sensitive optical imaging system (Photon Imager, Biospace Lab Inc., Paris, France) with 1 min acquisition time. No emission filter was used for acquisition. After obtaining *in vivo* images, mice were sacrificed with carbondioxide, and then lymph nodes were removed and subjected to another spectral fluorescence and BRET imaging session with the same settings.

2.3. Semiquantitative comparison of in vivo fluorescence imaging and in vivo BRET imaging

For semiquantitative image analysis, all procedures were performed with Maestro software (CRi Inc.) for spectral fluorescence images or M^3 Vision software (Biospace Lab Inc.) for BRET images. First, the resected lymph node which showed the highest signal on *ex vivo* spectral fluorescence image (quantum dot 655 spectrum) was defined as a standard lymph node, and then the relative signal intensities of each resected lymph node (S) were calculated as a ratio to the standard. The relative signal intensities of lymph nodes (I) were also calculated in *in vivo* spectral fluorescence and *in vivo* BRET images as a ratio to standard lymph nodes, which were same lymph nodes as defined in *ex vivo* images. Finally, the relative errors of both *in vivo* imaging methods from the *ex vivo* standards were calculated using the following formula: relative error = $|(S - I)/S|$. Statistical analyses were performed using a statistics program (GraphPad Instat, version 3.06, GraphPad Software, La Jolla, CA, USA) on a Windows computer. The Mann–Whitney test was performed to compare the mean relative errors between the fluorescence and BRET imaging. Values of $p < 0.05$ were considered statistically significant.

Supplementary Material

Refer to Web version on PubMed Central for supplementary material.

Acknowledgments

This research was supported by the Intramural Research Program of the NIH, National Cancer Institute, Center for Cancer Research.

References

1. Weissleder R, Pittet MJ. Imaging in the era of molecular oncology. Nature. 2008; 452:580–589. [PubMed: 18385732]
2. Tanaka E, Choi HS, Fujii H, Bawendi MG, Frangioni JV. Image-guided oncologic surgery using invisible light: completed pre-clinical development for sentinel lymph node mapping. Ann Surg Oncol. 2006; 13:1671–1681. [PubMed: 17009138]
3. Kim S, Lim YT, Soltesz EG, De Grand AM, Lee J, Nakayama A, Parker JA, Mihaljevic T, Laurence RG, Dor DM, Cohn LH, Bawendi MG, Frangioni JV. Near-infrared fluorescent type II quantum dots for sentinel lymph node mapping. Nat Biotechnol. 2004; 22:93–97. [PubMed: 14661026]

4. Kobayashi H, Hama Y, Koyama Y, Barrett T, Regino CA, Urano Y, Choyke PL. Simultaneous multicolor imaging of five different lymphatic basins using quantum dots. Nano Lett. 2007; 7:1711–1716. [PubMed: 17530812]
5. Hayashi K, Jiang P, Yamauchi K, Yamamoto N, Tsuchiya H, Tomita K, Moossa AR, Bouvet M, Hoffman RM. Real-time imaging of tumor-cell shedding and trafficking in lymphatic channels. Cancer Res. 2007; 67:8223–8228. [PubMed: 17804736]
6. Hoffman RM. The multiple uses of fluorescent proteins to visualize cancer in vivo. Nat Rev Cancer. 2005; 5:796–806. [PubMed: 16195751]
7. Yang M, Baranov E, Jiang P, Sun FX, Li XM, Li L, Hasegawa S, Bouvet M, Al-Tuwaijri M, Chishima T, Shimada H, Moossa AR, Penman S, Hoffman RM. Whole-body optical imaging of green fluorescent protein-expressing tumors and metastases. Proc Natl Acad Sci USA. 2000; 97:1206–1211. [PubMed: 10655509]
8. Yang M, Luiken G, Baranov E, Hoffman RM. Facile whole-body imaging of internal fluorescent tumors in mice with an LED flashlight. Biotechniques. 2005; 39:170–172. [PubMed: 16116787]
9. Levenson RM, Mansfield JR. Multispectral imaging in biology and medicine: slices of life. Cytometry A. 2006; 69:748–758. [PubMed: 16969820]
10. Xia Z, Rao J. Biosensing and imaging based on bioluminescence resonance energy transfer. Curr Opin Biotechnol. 2009; 20:37–44. [PubMed: 19216068]
11. So MK, Xu C, Loening AM, Gambhir SS, Rao J. Self-illuminating quantum dot conjugates for in vivo imaging. Nat Biotechnol. 2006; 24:339–343. [PubMed: 16501578]
12. Hama Y, Koyama Y, Choyke PL, Kobayashi H. Two-color in vivo dynamic contrast-enhanced pharmacokinetic imaging. J Biomed Opt. 2007; 12:034016. [PubMed: 17614724]
13. Hama Y, Koyama Y, Urano Y, Choyke PL, Kobayashi H. Two-color lymphatic mapping using Ig-conjugated near infrared optical probes. J Invest Dermatol. 2007; 127:2351–2356. [PubMed: 17522707]
14. Kobayashi H, Koyama Y, Barrett T, Hama Y, Regino CA, Shin IS, Jang BS, Le N, Paik CH, Choyke PL, Urano Y. Multimodal nanoprobes for radionuclide and five-color near-infrared optical lymphatic imaging. ACS Nano. 2007; 1:258–264. [PubMed: 19079788]
15. Kosaka N, Ogawa M, Sato N, Choyke PL, Kobayashi H. In vivo real-time, multicolor, quantum dot lymphatic imaging. J Invest Dermatol. 2009; 129:2818–2822. [PubMed: 19536144]
16. Xing Y, So MK, Koh AL, Sinclair R, Rao J. Improved QD-BRET conjugates for detection and imaging. Biochem Biophys Res Commun. 2008; 372:388–394. [PubMed: 18468518]

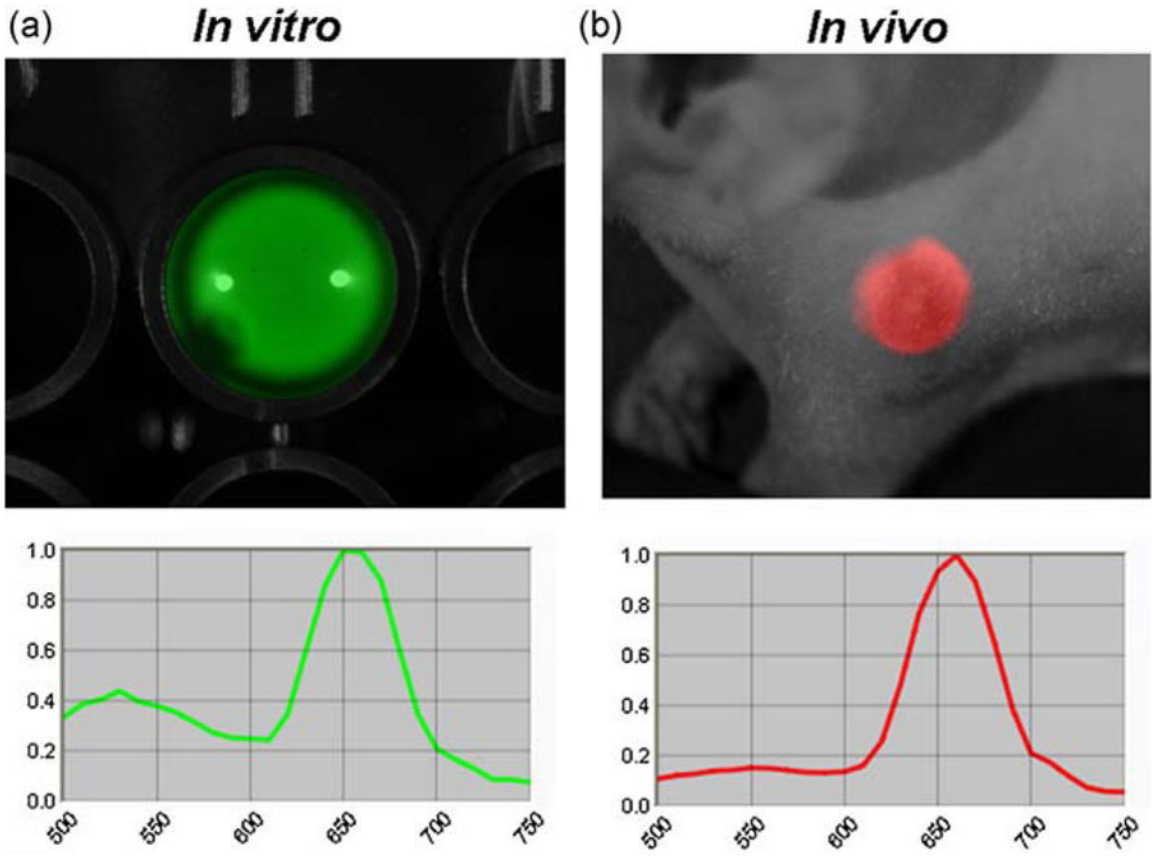

Figure 1.

Emission light spectra of BRET-Qdot655 excited by the incubation with coelenterazine in *in vitro* (a) and *in vivo* (b). Two emission peaks from bioluminescence (luciferase) and BRET (Qdot655) are identified *in vitro*; however, only one peak from BRET signal (Qdot655) is detected *in vivo*. Note that a mixture of BRET-Qdot655 and coelenterazine was injected subcutaneously for *in vivo* BRET spectral imaging. Also note that the emission peak from bioluminescence is shifted to longer wavelength because of the 515 nm long-pass emission filter.

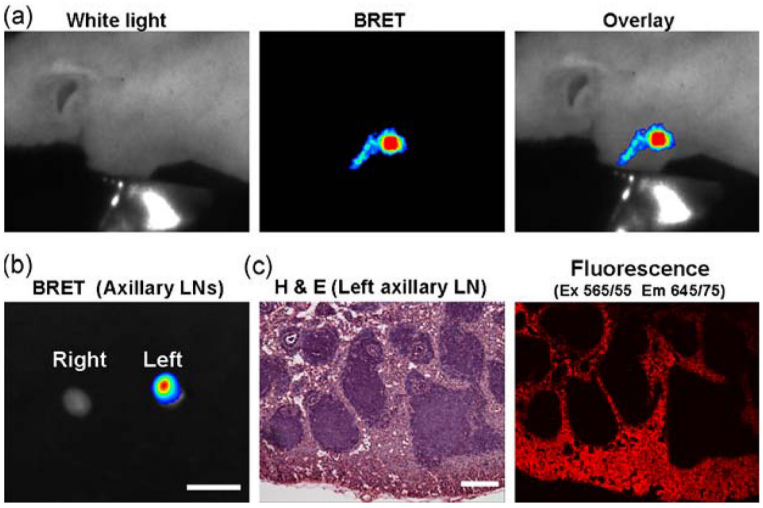

Figure 2.

BRET lymphatic image of the mouse receiving BRET-Qdot655 injection at the left paw. *In vivo* image demonstrates lymphatic duct and lymph node (a). Accumulation of BRET-Qdot655 in lymph node was confirmed by *ex vivo* imaging (b) and histological analysis (c). Bars on *ex vivo* image and H&E image are 5 mm and 100 μm, respectively.

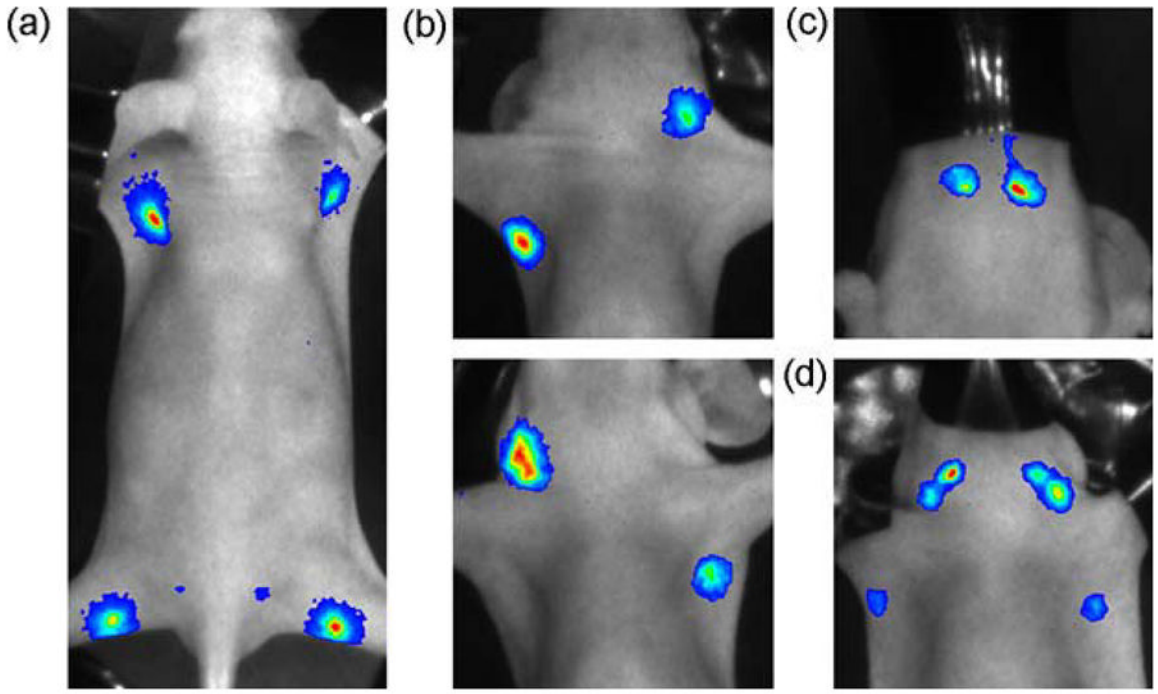

Figure 3.
BRET lymphatic images of different lymphatic basins. BRET-Qdot655 were injected at all four paws (a), the ear and forepaw (b), the chin (c), or five different sites (d: both forepaws, both ears and chin).

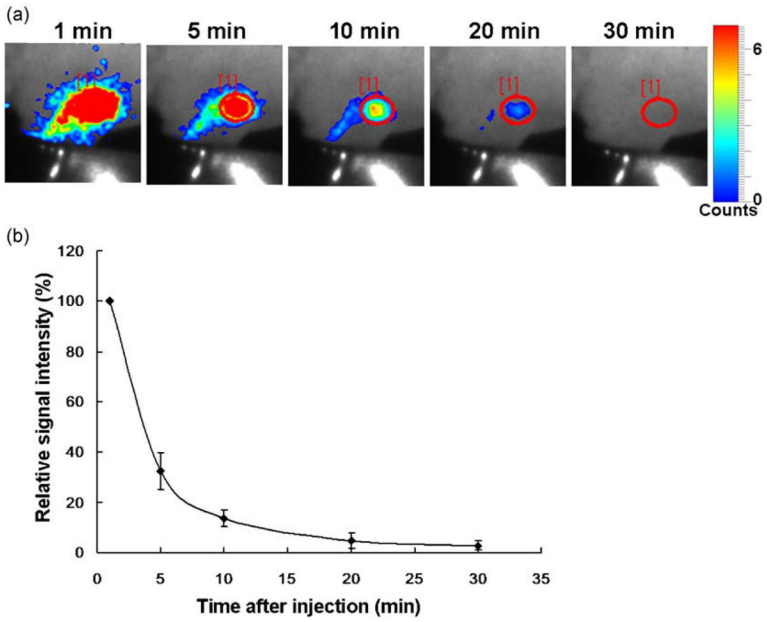

Figure 4.

Dynamic serial images of BRET lymphatic imaging in a mouse receiving BRET-Qdot655 injection at the left paw (a). Graph of relative signal intensity (n =3, 100% at 1 min) shows that BRET signal rapidly decreases with time (b). Note that the same scale, adjusted for the 10 min image, is used for all images.

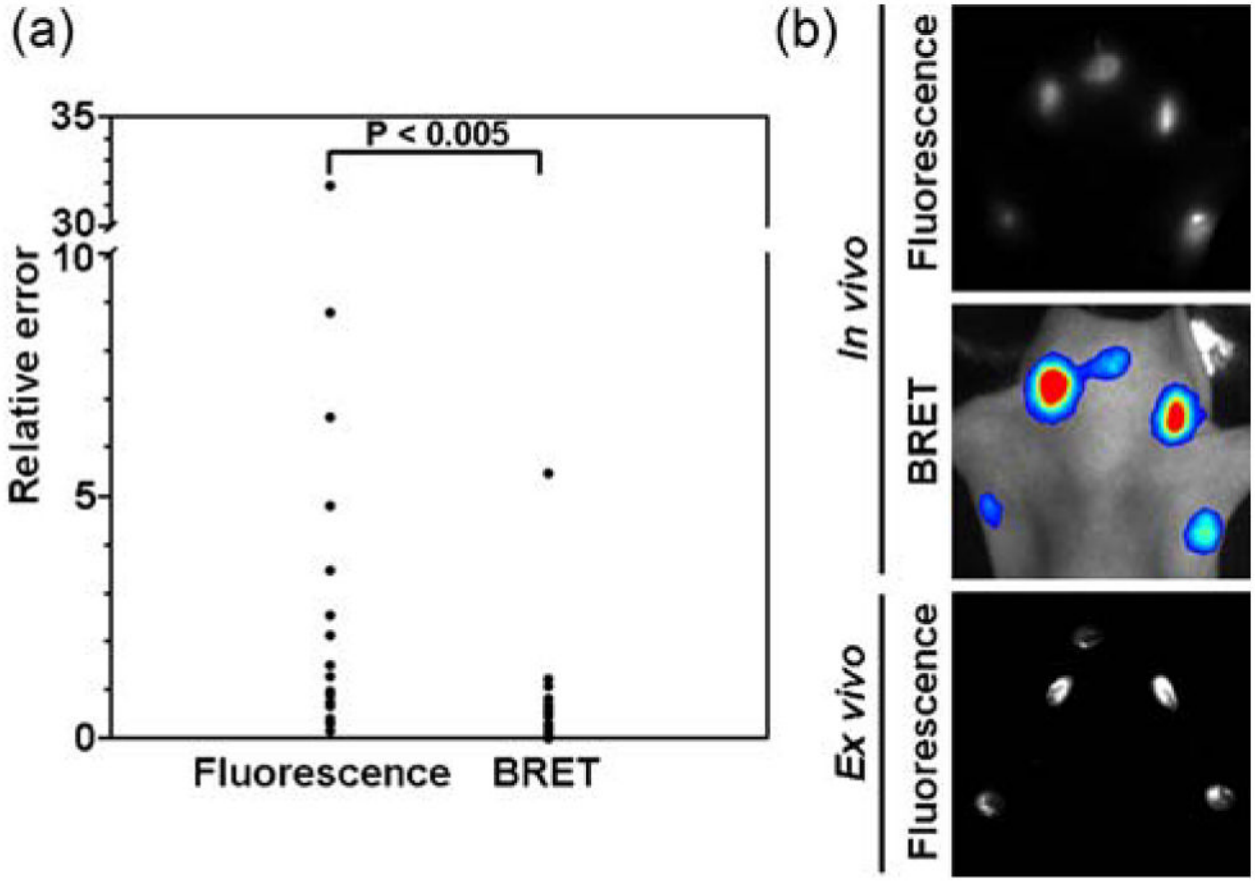

Figure 5.

Scatter plots (left) of the relative errors of *in vivo* fluorescence imaging and *in vivo* BRET imaging (a: n =17), when *ex vivo* fluorescence images of resected lymph nodes are used as gold standards. The relative error of *in vivo* BRET imaging (0.77 ± 1.27, average ± SD) is statistically lower than that of *in vivo* fluorescence imaging (4.04 ± 7.58). Representative images of five-site injected mice (both forepaws, both ears, and chin) are also shown (b). A representative image set shows that *ex vivo* fluorescence imaging correlated better with the *in vivo* BRET image than with the *in vivo* fluorescence image.